

**NUCLEAR ENERGY RESEARCH INITIATIVE (NERI) PROGRAM
DE-FG03 -99SF21884
TECHNICAL PROGRESS REPORT**

Fourth Quartile 1999
(Period 10/1/99 – 12/31/99)

Status Summary of NERI Tasks – Phases 1-3:

Phase 1:

Milestone/Task Description	Plan Completion Date	Actual Completion Date
Definition of the Environment	4/30/2000	
Continued Model Development	1/31/2002	
Measurements of Key Model Parameters	4/30/2002	

RECEIVED

Narrative:

FEB 07 2000

Task: 1. Definition of the Environment

OSTI

1. Task status:

During the past quartile we have explored the thermodynamics of various metal hydroxide and oxyhydroxide dehydration reactions of iron, nickel, and chromium with the objective of estimating the critical temperature, T_{cr} . This is the temperature at which the oxide is in equilibrium with the oxyhydroxide or hydroxide and water vapor under the expected repository conditions of temperature and pressure. Because localized corrosion requires the presence of an ionically conducting phase on the surface (to support oxygen reduction) T_{cr} is also the temperature below which "wet" corrosion first becomes possible. Past analyses have assumed that wet corrosion requires the presence of a layer of "bulk" water on the surface and hence that corrosion is not possible at temperatures above the boiling temperature of bulk water under the prevailing atmospheric pressure. Furthermore, significant elevation of the boiling temperature may occur if the aqueous phase becomes concentrated in salts. Because of the hydration of hygroscopic corrosion products, which may occur at significantly higher temperatures than the boiling temperature of water, and because of boiling temperature elevation effects, the past assumption needs to be reevaluated. This is the primary goal of this work.

We are addressing this issue primarily through thermodynamic calculation, using data that are available in various compilations (databases). Although extensive data are available for the oxides, only approximate and often incomplete data are available for the hydroxides and oxyhydroxides. This, no doubt, reflects the fact that the hydroxides and

DISCLAIMER

This report was prepared as an account of work sponsored by an agency of the United States Government. Neither the United States Government nor any agency thereof, nor any of their employees, make any warranty, express or implied, or assumes any legal liability or responsibility for the accuracy, completeness, or usefulness of any information, apparatus, product, or process disclosed, or represents that its use would not infringe privately owned rights. Reference herein to any specific commercial product, process, or service by trade name, trademark, manufacturer, or otherwise does not necessarily constitute or imply its endorsement, recommendation, or favoring by the United States Government or any agency thereof. The views and opinions of authors expressed herein do not necessarily state or reflect those of the United States Government or any agency thereof.

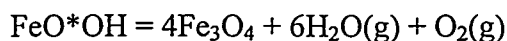
DISCLAIMER

Portions of this document may be illegible in electronic image products. Images are produced from the best available original document.

oxyhydroxides are often difficult to characterize and are frequently difficult to obtain in a dry state in a well defined crystalline form.

2. Issues/Concerns

We have now completed extensive calculations of T_{cr} for various hydroxides, oxyhydroxides, and oxides in the Fe-Cr-Ni system. The maximum value of T_{cr} at which a stable oxyhydroxide can exist under the conditions of the Yucca Mountain repository (≈ 6000 ft above the sea level and a relative humidity of 100 %) is 366°C . This temperature corresponds to the equilibrium temperature of the chemical reaction



Iron (III) oxyhydroxide, FeO^*OH , is almost certainly a proton conductor in the presence of "bound" water (although we have not yet found any definitive information on the subject in the literature) and hence is expected to support both general and localized corrosion. Accordingly, the possibility that corrosion initiates and propagates at temperatures significantly above the boiling temperature of water cannot be ignored.

In future, we will extend our analysis to the mixed oxides, for example, NiFe_2O_4 , which are known to form on alloys.

Task: 2. Continued Model Development:

1. Task status:

During the past quartile we concentrated our attention on the problem of the nucleation of cracks from corrosion pits.

2. Issues/Concerns:

As indicated by available experimental data, the nucleation of corrosion crevices (stress corrosion cracks and corrosion fatigue cracks) depends on two criteria: (1) The stress intensity factor for the crevice, K_I (or ΔK_I for corrosion fatigue), must exceed the threshold stress intensity factor, $K_{I,SCC}$ (or $\Delta K_{I,th}$), and (2) the crack growth rate must exceed the pit growth rate. However, in accordance with the slip dissolution model, the crevice tip is partially blocked by the passive film. Accordingly, for a given set of tip conditions (metal potential, pH, etc.), the anodic dissolution rate of the crevice tip must be smaller (estimations show that it must be much smaller) than the pit propagation rate (with the bare tip surface). This means that if the environmental component of the crack propagation rate is comparable with the mechanical component of the rate, the transition from a pit into a crevice occurs if: (1) the depth of the pit exceeds some critical length, L_{cr} , (where $K_I > K_{I,SCC}$ or $\Delta K_I \geq \Delta K_{I,th}$), and (2) the pit has passivated (i.e., died).

Because, for a given value of the stress, σ , the threshold stress intensity factor, K_I ($\Delta K_{I,th}$), depends not only on the pit depth, but also on the shape of the pit, it is important

to determine the shape of the pit as a function of its depth. During this quartile we developed a computer code for solving Laplace's equation for the electrostatic potential within a corroding cavity. This was done by using the boundary element method for an open pit of arbitrary axis-symmetrical geometry under a thin electrolyte film covering the external surface and by assuming arbitrary polarization laws for the electrochemical reactions occurring inside and outside the pit. Using this program to calculate the current and potential distributions, together with Faraday's law, yields the shape of the pit as a function of its age, and, accordingly, the shape of the pit as a function of its depth. However, our experimental investigations show that the pits on Alloy C-22 are covered with an oxide film (closed pits), which is presumably the remnant of the barrier layer. Our code is now being generalized to handle the case of a closed pit.

We began to develop a computer code to calculate the crevice (pit and crack) growth rate under thin electrolyte film. The model takes into account cathodic processes that occur on the sides of the crevice and on the external surfaces (outside the crevice).

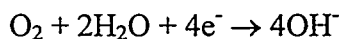
Finally, we have also initiated the development of computer code for calculating the corrosion potential (on the basis of the Mixed Potential Model) for Alloy C22 when covered by the thin electrolyte film.

Task 3: Measurements of Key Model Parameters:

Anodic (in the potential range from the steady-state potential to more positive values) and cathodic (at potentials more negative than the steady-state potential) potentiodynamic curves (current density vs. potential, at a potential sweep rate of 1 mV/s) were measured on Alloy C-22 alloy in NaCl solutions (from 0.1 to 1.0 M) at temperatures from 20 to 95°C. These measurements are being performed under subcontract to SRI by the Frumkin Institute in Moscow, Russia.

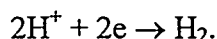
- **Cathodic Curves**

A region of oxygen reduction with the limiting current for the reaction



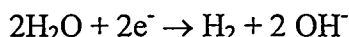
is observed in the cathodic curve. This region lies at potentials that are more negative than approximately -0.1 V (SHE), i.e. significantly more negative than the equilibrium potential for the oxygen electrode reaction for the prevailing concentration of oxygen dissolved in water [0.815 V (SHE) at pH = 7]. Therefore, the formally determined exchange current (i_0) of this reaction (by the extrapolation of the observed Tafel region to the equilibrium potential) is very low ($i_0 < 10^{-10}$ A/cm²), as expected. In the future, the value of i_0 will be refined and measured as a function of important independent variables ([O₂], pH, T). The limiting current for oxygen reduction is virtually independent of pH within the range from pH = 6 to 10.

At pH < 6, the cathodic polarization curve displays a segment corresponding to the hydrogen evolution reaction



The region of the limiting current for hydrogen evolution almost coincides with the region of the limiting current for oxygen reduction. The limiting current of hydrogen reduction increases as the pH is decreased, as expected. At current densities lower than the limiting value, a Tafel region is observed with a slope of 130 mV/decade. The extrapolation of the Tafel slopes to the equilibrium potential allows us to estimate the exchange current i_0 of this reaction: at 20 °C, for 0.1 M NaCl solution with pH = 2, i_0 is 2×10^{-5} A/cm²; at pH = 3, i_0 is 6×10^{-6} A/cm²; at 80 °C, for 0.1 M NaCl solution with pH = 3, i_0 is 5×10^{-5} A/cm².

At more negative potentials, the reaction



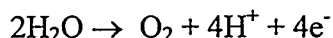
takes place. It is not yet known whether kinetic parameters can be measured for this reaction as well.

• Anodic Curves

The anodic polarization curves of current density vs. potential consist of several segments. The curve segment in the vicinity of the steady-state potential may be ascribed to "pseudoactive" alloy dissolution. In this region, the alloy dissolution rate increases with the potential; however, this process is, probably, hampered by partial passivity. Obviously, at the steady-state potential in neutral NaCl solutions, the alloy is covered with natural oxide film preventing active dissolution.

At higher potentials, a region is observed, which we will call "the passivity region". In this region, the current increases with the potential, with the slope being low and in some cases zero (parallel to the potential axis) or even negative. In this passive region, the current increases with an increase in temperature and with an increase in the concentration of NaCl. At pH = 11, two current waves are observed instead of the passive region. The waves may be caused by the dissolution of the alloy components to form oxidation products that are readily soluble alkaline solutions. These components include molybdenum (13.26% in the alloy), tungsten (2.80%), and chromium (21.70%).

At the most positive potentials, an abrupt increase in the current with increasing potential is observed; this is associated, probably, with transpassivation. At these potentials, the oxygen evolution reaction



may proceed; however, no gas-bubble formation was observed on the electrode.

The complicated anodic behavior of the alloy at ambient temperature (very short segment of "pseudoactive" dissolution with an uncertain slope, possibly due to the presence of natural oxide film on the metal) does not allow us to easily determine with certainty the kinetic parameters of the metal dissolution reaction. At high temperatures (80 and 95 °C) and high concentrations (1 M NaCl), however, the region of "pseudoactive" dissolution is wider. Here, the Tafel slope may be estimated to be 140 mV/decade.

- **Pitting**

The initiation of pitting was studied under potentiodynamic/potentiostatic conditions. Preliminary experiments involved sweeping the potential from the steady-state value to a (more positive) value of interest at a sweep rate of 5 mV/s. Then, the electrode potential was held at the final potential for 1200 s, while measuring the time variation of the current. All experiments were performed on Alloy C-22.

The study, which was performed in 0.1 and 0.2 M NaCl solutions at 20 °C, allowed us to make the following conclusions. With increasing anodic potential, two competitive processes proceed on the alloy surface: on the one hand, the growth of the oxide film enhances alloy passivation, and, on the other hand, an increase in the aggressive effect of chloride ions leads to passivity breakdown and the initiation of pitting. At a comparatively small potential shift from the steady-state value in the positive direction, the second effect prevails and reaches a maximum at a potential of about 0 V (SHE) [the steady-state potential was about -0.15 V (SHE)]. Examination of the surface with a metallographic microscope with the oxide film intact showed the presence of great number (tens) of pit. However, removal of the passive film changed the situation. Only a small number of pits were found in the metal. They, probably, correspond to the current peaks, in which the largest charges passed (according to the preliminary data, more than 25 μC). Thus, many of the "pits" observed with the film intact were, in fact, imperfections in the passive film, most likely in the outer layer.

After electrode exposure at higher potentials (in the passivity region), only a few, small current peaks were observed on the current vs. time curve. Several small pits formed on the metal; the total decrease in the current during the course of the experiment indicated that the pits are, most probably, metastable. In some experiments, neither current peaks nor pits on the metal were observed.

At the potential of the transpassive increase in the current, the electrode surface, when viewed after the experiment, was found to be covered with a thick brown oxide film. Upon the removal of the film with fine emery paper (for example, in the experiment at a potential of 1.25 V), numerous pits of various size and depth were seen on the surface. At the beginning of the experiment at a potential of 1.25 V (SHE), the current was high (significantly higher than at the potentials in the passivity region), but it decreased significantly with time. Probably, this was caused by the blocking of the pits, which had formed at high currents, with growing oxide (film closed pits).

Cost Performance:

